CHAPTER 3

Kinetic and thermodynamic studies of sagwan sawdust pyrolysis for its bioenergy potential

3.1 Introduction

Fossil fuel (coal, petroleum or natural gas) resources are finite and it's a matter of time when they run out. In addition to concern over the decline in fossil fuel resources, the increasing demand for energy and deterioration in environmental condition due to the rapid utilization of easily accessible fossil fuels have resulted in an increase in research for sustainable, renewable and alternative energy sources (Celaya et al., 2017; Guan et al., 2015). Lignocellulosic biomass is widely available and considered as a potential renewable energy source in the future. India meets 70% of its energy requirement using fuel woods and in the process, around 50 million tonnes of wood are removed from forests every year (Annual report, 1995-96). According to FAO (2001), a total global sagwan plantations of 5.7 million hectares (3 % of total forest plantations) was recorded and of which about 92 % sagwan plantation estate is in Asia including 43 % in India. In India, an average yield of 172 m^3/hectare with an MAI (mean annual volume increment) of about 2.46 m^3/hectare/year was reported by FAO (1985). According to Bhat and Ma,

(2004), India covers 2450000-hectare extent of sagwan plantations and MAI of 2-7 m^3/hectare/year. Annually, a huge amount of sagwan sawdust (SS), a lignocellulosic biomass is produced after making furniture, wood decorative and other things. These left over residues have no economic usage and are large in volume creating disposal problem. Thus utilization of this waste for biofuel (syngas, bio-oil or biochar) production via thermochemical process is a promising energy conversion technique. Various thermochemical techniques include pyrolysis, gasification, combustion or liquefaction (Sharma et al., 2015). Among them, pyrolysis is one of the most employed methods, operated in absence of oxygen, to convert biomass into biofuel and various useful chemicals using technologies of fixed bed, fluidized bed, auger, sprout bed etc. (Bridgwater and Peacocke, 2000). So, for a better understanding of pyrolytic cracking reaction mechanism and conversion process, the study of kinetics and thermodynamics is very important. In addition to it, biomass pyrolysis kinetics is important to assess biomass as feedstock for fuel or chemical production and productive design and control of thermochemical process. TGA has been proved to be a dynamic approach for biomass pyrolytic kinetic study. TGA measures the amount and rate of change in the weight of biomass as a function of temperature or time, in an inert atmosphere (El-Sayed and Mostafa, 2015). The weight losses observed during TGA reflects the physical and chemical structure changes occurring during the conversion process. The type of biomass, properties of their organic content and the environment in which thermal decomposition takes place affect the thermal decomposition rate and also the activation energy.

The objective of this study was to investigate SS as a potential source of bio-energy because they are environmental friendly and provide a sustainable energy source. The physical and chemical characteristics of biomass were assessed for proximate analysis,

elemental analysis, compositional analysis and HHV. TG experiments were performed at three different heating rates (5, 10 and 20 ˚C/min) to investigate the thermal degradation behaviour and reaction kinetics of SS under inert condition. Kinetic and thermodynamic parameters for the process were obtained via iso-conversional model free FWO, KAS and Friedman models using TGA results.

3.2 Experimental

3.2.1 Raw material

SS was used as the raw material for the research work. It was collected from local sawmill located in the vicinity of Banaras Hindu University campus, Varanasi, India. Collected SS was rinsed twice with double distilled water to remove the impurities adhered on its surface and were kept in the sunlight for 4 days and then in an air oven at 105 ˚C till we get the constant weight. SS was then sieved (-60 mesh +85 mesh) to get the particle size in the range of 0.18 - 0.25 mm for the experiment. The prepared sample was sealed in sample bottles and kept in the desiccator at room temperature for the experiments.

3.2.2 Chemicals and reagents

All the reagents and chemicals used for the research work were of analytical grade and the solutions were prepared with double distilled water (DDW).

Reagents for neutral detergent fiber analysis

Neutral detergent solution (1 L): Sodium borate decahydrate 6.81 g, disodium ethylene diamine tetraacetate 18.61 g, sodium lauryl sulfate 30 g, 2- ethoxyethanol 10 mL, disodium phosphate anhydrous 4.56 g, DDW 1000 mL, sodium sulphite and acetone

Reagents for acid detergent fiber analysis

Acid detergent solution (1 L): Sulphuric acid (1 N) 1L, cetyltrimethylammonium bromide (CTAB) 20 g, acetone

Reagents for lignin estimation

Saturated potassium permanganate (1 L): DDW 1 L, $KMnO_4$ 50 g, Ag_2SO_4 0.05 g. Lignin buffer solution (1 L): Ferric nitrate nonahydrate 6 g, silver nitrate 0.15 g, acetic acid glacial 500 mL, potassium acetate 5 g, tertiary butyl alcohol 400 mL, distilled water 100 mL. Combined permanganate solution: two parts of saturated potassium permanganate solution were diluted with one part of lignin buffer solution. Demineralising buffer (1 L): Oxalic acid dihydrate 50 g, 95 % ethanol 700 mL, concentrated HCl (12 N) 50 mL, DDW 250 mL, ethanol 80 % and acetone.

3.2.3 Analytical techniques for SS characterization

SS was characterized for its proximate analysis, elemental analysis, compositional analysis and HHV. ASTM protocols were used for the determination of MC, VM and AC. FC was determined taking the difference as shown in eq. 3.1.

$$FC = [100 - (MC+VM+AC)] \% \quad (3.1)$$

Elemental analysis of SS was done using elemental analyser (EURO EA, EURO ECTOR instruments and software, Italy) to get the weight percentage of Carbon (C), hydrogen (H), nitrogen (N) and sulphur (S). The weight percentage of oxygen (O) was calculated by taking the difference as shown in eq. 3.2.

$$O = [100 - (C+H+N+S)] \% \quad (3.2)$$

Compositional analysis of SS was done following the methods of Van Soest to calculate the amount of hemicellulose, cellulose and lignin. In Van Soest analysis, SS was separated into NDF (Neutral detergent fibre) by treating with neutral detergent solution and ADF (Acid detergent fibre) by treating with acid detergent solution. NDF contains hemicelluloses, cellulose, lignin and ash whereas ADF contains cellulose, lignin and ash. By subtracting ADF from NDF, hemicellulose was calculated. Again by treating ADF with potassium permanganate and buffer solution (2:1), lignin gets solubilized

while cellulose and ash remain as insoluble residue. From here, lignin was calculated by substracting the insoluble residue from ADF. Further cellulose was separated and calculated by ashing the insoluble residue.

HHV of SS was determined using bomb calorimeter (Rajdhani Scientific, NSTTS Co., New Delhi, India) by taking 1 g sample following ASTM standard.

3.2.4 TG experimental process

TG experiments were performed to study thermal degradation behaviour of SS by using thermogravimetric analyzer (NETZSCH 449 F3 Jupiter, Germany). The experiments were performed at three different linear heating rates of 5, 10 and 20 ˚C/min using the particle size in the range of 0.18 – 0.25 mm under non-isothermal condition to study the effect of temperature and heating rate on thermal degradation behaviour. All the experiments were performed in an inert atmosphere with continuous purging of nitrogen gas (99.99 % purity) at the flow rate of 60 mL/min. The experiments were started at ambient temperature and the temperature was raised up to 900 ˚C. The differential thermogravimetric (DTG) results were obtained taking the derivative of TG results.

3.2.5 Kinetic and thermodynamic study

The physico-chemical characteristics of biomass varies from one to another and thus, different biomass shows different pyrolytic behaviour, which makes pyrolysis a complex process (Sriram and Swaminathan, 2018; Huang et al., 2016). TG and DTG data were used to calculate the kinetic and thermodynamic parameters for SS degradation. The general pyrolysis reaction can be symbolized by the eq. 3.3.

$$\text{Biomass} \rightarrow \text{Volatiles (condensable + non-condensable)} + \text{Biochar} \quad (3.3)$$

Biomass degradation process is considered as single reaction (Vyazovkin et al., 2011) and it consists of heterogeneous solid state reactions, where reaction kinetics is described by eq. 3.4 as mentioned below.

$$\frac{d\alpha}{dt} = k\,(T)\,.\,f\,(\alpha) \tag{3.4}$$

Where, T is the temperature, t is the reaction time, k (T) is the reaction rate constant dependent on temperature, α is the fractional conversion and f(α) is the function of conversion (El-Sayed and Mostafa, 2015).

Fractional conversion is described by the expression appended below.

$$\alpha = \left(\frac{W_o - W_t}{W_o - W_f}\right) \tag{3.5}$$

Where, W_o is the initial mass of the sample, W_t is the instantaneous mass of the sample at time t and W_f is the mass of the sample at the end of the process. The k(T) is the reaction rate constant and is described by the Arrhenius equation.

$$k\,(T) = A.\ e^{\frac{-E}{RT}} \tag{3.6}$$

Where, A is the pre-exponential factor in min^{-1}, E is the activation energy in (J/mol), and R is the universal gas constant 8.314 J/(mol.K). Linear heating rate, β, is defined as

$$\beta = \frac{dT}{dt} \tag{3.7}$$

Combining of equations 3.4 and 3.6 gives the fundamental equation 3.8 for the analytical method to determine kinetic parameters, on the basis of TG data.

$$\frac{d\alpha}{dt} = A.\ e^{\frac{-E}{RT}}.\ f\,(\alpha) \tag{3.8}$$

From equations 3.7 and 3.8, equation 3.9 can be formed as:

$$\frac{d\alpha}{dT} = \frac{A}{\beta}.\ e^{\frac{-E}{RT}}.\ f\,(\alpha) \tag{3.9}$$

Arranging both side of equation 3.9 and then integrating,

$$g\,(\alpha) = \int_0^{\alpha} \frac{d\alpha}{f(\alpha)} = \frac{A}{\beta}\int_{T_0}^{T} e^{\frac{-E}{RT}}\,dT \tag{3.10}$$

Where, g (α) is a function of conversion α and algebraic expression f (α) is related to the physical model which describes the solid state reaction kinetics. Different forms of f (α) and g (α) that represent different reaction mechanism are presented in Table 3.1. These

equations can be used to predict the reaction mechanism for SS degradation, revealed by the TG curves. In this work, E was calculated from non-isothermal TG/DTG analysis. Iso-conversional models were used for the determination of kinetic parameters from plots at same level of conversion at different heating rates.

3.2.6 Iso-conversional models

Thermal degradation of biomass is a complex process where multiple reactions occur simultaneously with different rates. Thus, these complex reactions cannot be described by simple kinetic model. To inspect the in-depth analysis of thermal decomposition of biomass, iso-conversional models are often used. These methods require TG data at least at three different heating rates. In this study, three different iso-conversional models FWO, KAS and Friedman model (Baray Guerrero et al. 2016) were followed to determine the kinetic parameters.

3.2.6.1 FWO model

FWO is an integral iso-conversional technique for determination of E for each value of conversion derived from equation 3.8 using Doyle's approximation. FWO equation as described by the eq. 3.11 is shown below:

$$\ln \beta_i = \ln\left(\frac{A.E}{R.g(\alpha)}\right) - 5.331 - 1.052\left(\frac{E}{R.T}\right) \quad (3.11)$$

The plot of ln β vs $\left(\frac{1}{T}\right)$ at three different rates for each conversion is a linear relation and slope of which gives $-1.052\frac{E}{R}$ and E is calculated.

3.2.6.2 KAS model

Similar to FWO, KAS is also an integral iso-conversional method to determine the E required for the process at different conversion, based on the following eq. 3.12:

$$\ln\left(\frac{\beta}{T^2}\right) = \ln\left(\frac{A.E}{R.g(\alpha)}\right) - \frac{E}{RT} \quad (3.12)$$

The above expression follows the equation of a straight line and from the plot of ln $\left(\frac{\beta}{T^2}\right)$ vs $\frac{1}{T}$ at three different rates for each conversion, the slope is equal to - $\frac{E}{R}$ to calculate the E.

3.2.6.3 Friedman model

Friedman is a differential iso-conversional technique to calculate the E as given by the eq. 3.13 mentioned below:

$$\ln\left(\frac{d\alpha}{dt}\right) = \ln(A \,.\, f(\alpha)) - \left(\frac{E}{RT}\right) \tag{3.13}$$

The above equation is derived by taking natural logarithmic to equation 3.8. It is assumed that f (α) is constant and biomass degradation is independent of temperature and depends on the rate of mass loss. The plot of ln $\left(\frac{d\alpha}{dt}\right)$ vs $\frac{1}{T}$ at three different rates for each conversion gives a series of straight line with slope $\left(\frac{-E}{R}\right)$ to calculate the E.

3.2.7 Prediction of reaction mechanism

The reaction model for solid state reactions during thermal degradation of SS was explored by Z-master plot in association with Criado method (Criado, 1978). Master plots are the theoretical plots which are dependent on the kinetic model of the reaction but they are not dependent on other kinetic parameters like A and E (Dhyani et al., 2017). The below equation 3.14 was used to create the master plots (theoretical and experimental) equivalent to various solid-state reaction mechanism as mentioned in Table 3.1.

$$\frac{Z(\alpha)}{Z\,(0.5)} = \frac{f(\alpha)\times g(\alpha)}{f(0.5)\times g(0.5)} = \left(\frac{T_\propto}{T_{0.5}}\right)^2 \times \frac{(d\alpha/dT)\alpha}{(d\alpha/dT)0.5} \tag{3.14}$$

From the above equation, the term $\frac{f(\alpha)\times g(\alpha)}{f(0.5)\times g(0.5)}$ provides the theoretical curves related to the characteristics of each reaction mechanism whereas the expression $\left(\frac{T_\propto}{T_{0.5}}\right)^2 \times$

$\frac{(d\alpha/dT)\alpha}{(d\alpha/dT)0.5}$ gives the experimental curve. The conversion value α = 0.5 was chosen as the reference point at which the curves from all the theoretical and experimental data will intersect at $\frac{Z(\alpha)}{Z(0.5)}$. The appropriate reaction mechanism for experimental value was selected by comparing the theoretical and experimental curves. The theoretical curve which is closer to the experimental curve was chosen as the reaction mechanism for the degradation process (Dhyani et al., 2017).

Table 3.1 Different kinetic models for solid state kinetics

Solid state process	**Mechanism**	**f(α)**	**g(α)**
1-D diffusion	D1	$1/2^{\alpha}$	α^2
2-D diffusion	D2	$[-\ln(1-\alpha)]^{-1}$	$(1-\alpha)\ln(1-\alpha)+\alpha$
3-D diffusion (Jander)	D3	$3/2(1-\alpha)^{2/3}[1-(1-\alpha)^{1/3}]^{-1}$	$[1-(1-\alpha)^{1/3}]^2$
3-D diffusion (Ginstlinge)	D4	$3/2[(1-\alpha)^{1/3}-1]^{-1}$	$1-2/3\alpha-(1-\alpha)^{2/3}$
Contracting cylinder	F2	$2(1-\alpha)^{1/3}$	$1-(1-\alpha)^{1/2}$
Contracting sphere	F3	$(1-\alpha)^{2/3}$	$1-(1-\alpha)^{1/3}$
Power Law	P2/3	$2/3\alpha^{-1/2}$	$\alpha^{3/2}$
Power Law	P2	$2\alpha^{1/2}$	$\alpha^{1/2}$
Power Law	P3	$3\alpha^{2/3}$	$\alpha^{1/3}$
Power Law	P4	$4\alpha^{3/4}$	$\alpha^{1/4}$
Avrami-Erofeev	A1	$½(1-\alpha)[-\ln(1-\alpha)]^{1/3}$	$[-\ln(1-\alpha)]^{2/3}$
Avrami-Erofeev	A2	$2(1-\alpha)[-\ln(1-\alpha)]^{1/2}$	$[-\ln(1-\alpha)]^{1/2}$
Avrami-Erofeev	A3	$3(1-\alpha)[-\ln(1-\alpha)]^{2/3}$	$[-\ln(1-\alpha)]^{1/3}$

Avrami-Erofeev	A4	$4(1-\alpha)[-\ln(1-\alpha)]^{3/4}$	$[-\ln(1-\alpha)]^{1/4}$
1st order nucleation	R1	$(1-\alpha)$	$-\ln(1-\alpha)$
2nd order nucleation	R2	$(1-\alpha)^2$	$(1-\alpha)^{-1}-1$
3rd order nucleation	R3	$(1-\alpha)^3$	$1/2[(1-\alpha)^{-1}-1]$

3.2.8 Calculation of pre-exponential factor and thermodynamic parameter

Apart from the determination of kinetic parameters, calculation of pre-exponential factor and thermodynamic parameter is also necessary to define the feasibility of the process. E for the process was calculated using iso-conversional methods as described in section 3.3. However, the calculation of pre-exponential factor and reaction mechanism given by iso-conversional methods are not reliable (Dhyani et al., 2017). Thus, Kissinger method was used to calculate the pre-exponential factor as given by eq. 3.15 and thermodynamic parameters i.e. change in Gibbs free energy (ΔG), enthalpy (ΔH) and change in entropy (ΔS) were calculated using equation 3.16, 3.17 and 3.18, respectively (Kim et al., 2010). In this study, heating rate of 10 °C/min and E obtained from FWO model was used to calculate all the parameters.

$$A = (\beta . E . e^{\frac{E}{R.T_m}}) / RT_m^2 \quad (3.15)$$

$$\Delta G = E + R . T_m . \ln\left(\frac{K_B T_m}{h.A}\right) \quad (3.16)$$

$$\Delta H = E - RT \quad (3.17)$$

$$\Delta S = \frac{\Delta H - \Delta G}{T_m} \quad (3.18)$$

Where K_B is Boltzmann constant (1.381×10^{-23} J/K); h is Plank constant (6.626×10^{-34} Js) and T_m is the DTG peak temperature in K.

3.3 Results and Discussions

3.3.1 Physico-chemical properties of SS

Physical and chemical characteristics of SS are presented in Table 3.2. The proximate analysis confirmed low MC (2.47 %), high amount of VM (76.39 %) and moderate AC (4.92 %) that could be suitable for thermochemical conversion processes (pyrolysis, combustion or gasification). In biomass, chemical energy is stored mainly in the form of VM and FC (Akhtar et al., 2016). High AC in the biomass affects burning rate thus reducing energy conversion and can cause fouling or aggregation leading to poor combustion and disposal problem (Lacovidou et al., 2018). Elemental analysis result showed SS is rich in carbon (49.22%) and oxygen (44.49%) contents. It has 5.73% hydrogen, low nitrogen (0.56%) and sulphur content below detection range. Low nitrogen and sulphur content are extra advantageous because it will release less NO_x and SO_x. The disadvantages of high amount of SO_x and NO_x includes the formation of photochemical smog, acid rain, ground-level ozone etc. In addition, NO_x and SO_x also contribute to particulate matter (PM) in the air from aerosols formed and creates breathing and vision problem (Mladenovic et al., 2018). These all damages the human and animal health causing harm to the natural ecosystem. In addition, negligible sulphur indicates lower emission or corrosion. Sulphur in the biomass may combine with other elements in the biomass and may release toxic gases e.g. H_2S, SO_x, which are responsible for acid rain. The chemical composition of SS was done on dry basis. It consists of 51.6 % of cellulose, 13.6 % of hemicelluloses and 24.4 % of lignin which is in the range of lignocellulosic biomass.

The HHV of SS was calculated as 17.86 MJ/kg which is slightly higher than Mustard stalk (17.57 MJ/kg) (Maiti et al., 2007) and Tea waste (13.60 MJ/kg) (Parikh et al., 2005) but lower than that of smooth cordgrass (18.5 MJ/kg) (Liang et al., 2014). Thus,

SS can be an attractive biomass to be used as an alternative fuel since its HHV is higher as compared to other biomass available and HHV is the most significant properties of fuels which explain the higher energy content and determine the efficient use of biomass and fossil fuels (Acar and Ayanoglu, 2012).

Table 3.2 Physical and chemical characteristics of SS

Parameters	Results
Proximate analysis (wt. %)	
MC	2.47
VM	76.39
AC	4.92
FC*	16.22
Ultimate analysis (wt. %)	
C	49.22
H	5.73
N	0.56
O*	44.49
S	bdr
Atomic ratios	
H/C	1.40
O/C	0.68
(N+O)/C	0.69
Compositional analysis (wt. %)	
Hemicellulose	13.60
Cellulose	51.60
Lignin	24.40
Others	10.40
HHV (MJ/kg)	17.86

*By difference, bdr – below detection range

3.3.2 TG and DTG analysis

Non-isothermal TG experiments were performed at three different heating rates to evaluate the thermal degradation and kinetic parameters for SS devolatilization. TG and DTG curves at three different heating rates 5, 10 and 20 °C/min in nitrogen atmosphere are shown in Fig. 3.1 and 3.2, respectively. Like other biomass, SS is also a lignocellulosic biomass, which consists of different components (hemicellulose, cellulose and lignin) as confirmed by Van Soest method and each component of it has different degradation temperature range. Hemicellulose has casual amorphous nature and decomposes in the temperature range of 200 - 315 °C, cellulose is of crystalline nature and has long polymer of glucose units that degrades from 260 to 400 °C whereas lignin is a heavily cross-linked molecule that degrades over a wide range of temperature from 180 to 900 °C (Yang et al., 2007).

From Fig. 3.1, it can be ascertained that the whole TG curve can be divided into three different zones. Zone 1 was considered from ambient to 130 °C where a significant amount of mass loss 3 - 4 wt. % was observed with small peaks in the DTG curve at the approximate temperature below 125 °C. This early weight loss is attributed to the removal of MC and light organic VM from biomass. Thereafter, the degradation profile showed linear behavior till approximately 200 – 210 °C only with the release of lighter volatiles. Major devolatilization stage in thermochemical conversion of SS was observed in zone-II which continued till around 480 - 500 °C. The sudden decrease of around 65-70 wt. % was observed in this zone and thus, this zone of sawdust degradation was considered as active phase. Pyrolytic cracking occurred with simultaneous exothermic reactions. A wide range of volatiles were released in this region due to degradation of the polymeric fraction that constitutes the lignocellulosic biomass. This phase describes the degradation of all three components where breakage

of C - C bonds of carbon-containing compounds occurs. This was followed by slow weight loss in zone-III until temperature reached 900 °C, which is attributed to the decomposition of remaining lignin or biochar (Gomez et al., 2007). Nature of the DTG curve for 5 °C/min showed a slight deviation after around 280 °C; which showed completion of hemicellulose degradation because it is least stable to the polymeric structure in biomass, thereby decomposing at the earliest (Burhenne et al., 2013). The same change in two other DTG peaks was also observed but at higher temperature, i.e. at around after 295 °C for 10 °C/min and 300 °C for 20 °C/min, respectively. Maximum DTG peak for SS at different heating rates were in between 335 - 365 °C, which is mainly attributed to cellulose decomposition (Huang et al., 2016). Lignin volatilization occurred over a wide range of temperature from approximately 180 to 900 °C, but very small rate of weight loss was observed because it is harder to decompose. Small peak in the DTG curve in the temperature range 640 – 900 °C may be due to high rate of lignin degradation.

The effect of heating rate can be seen from TG, DTG and conversion curves depicted in Fig. 3.1, 3.2 and 3.3, respectively. The nature of all three curves did not change in appearance with increasing heating rate however, in the all the figures curve shifted to their right with the increase in heating rate which signifies pyrolysis temperature needed to get the same weight loss and conversion became higher. Xiang et al. (2016) found similar nature of the curves with poplar sawdust. This is because the time needed to attain the same reaction temperature will be shortened and thus, there is no adequate residence time for the volatiles evolving at that reaction temperature, hence higher temperature is needed for the decomposition process (Chen et al., 2015). The maximum devolatilization peak in the DTG curve shifted from around 340 °C at 5 °C/min to around 365 °C at 20 °C/min without any change in its nature. This could be because of

the decrease in the heat transfer efficiency at the higher heating rate. At lower heating rate, heating of biomass particle occurs more gradually and leads to better heat transfer to the inner parts of biomass (Biagini et al., 2006). The increase in heating rate leads to the maximization of breakdown rate of biomass because of increase in thermal energy that facilitates the heat transfer between the surrounding and the interior of the biomass sample (Caballero et al., 1997). Thus, the thermal degradation of chemical bonds in the sawdust produces condensable vapors (organic compounds) and non-condensable fractions (e.g. H_2, CO, CO_2, CH_4) (Neves et al., 2011).

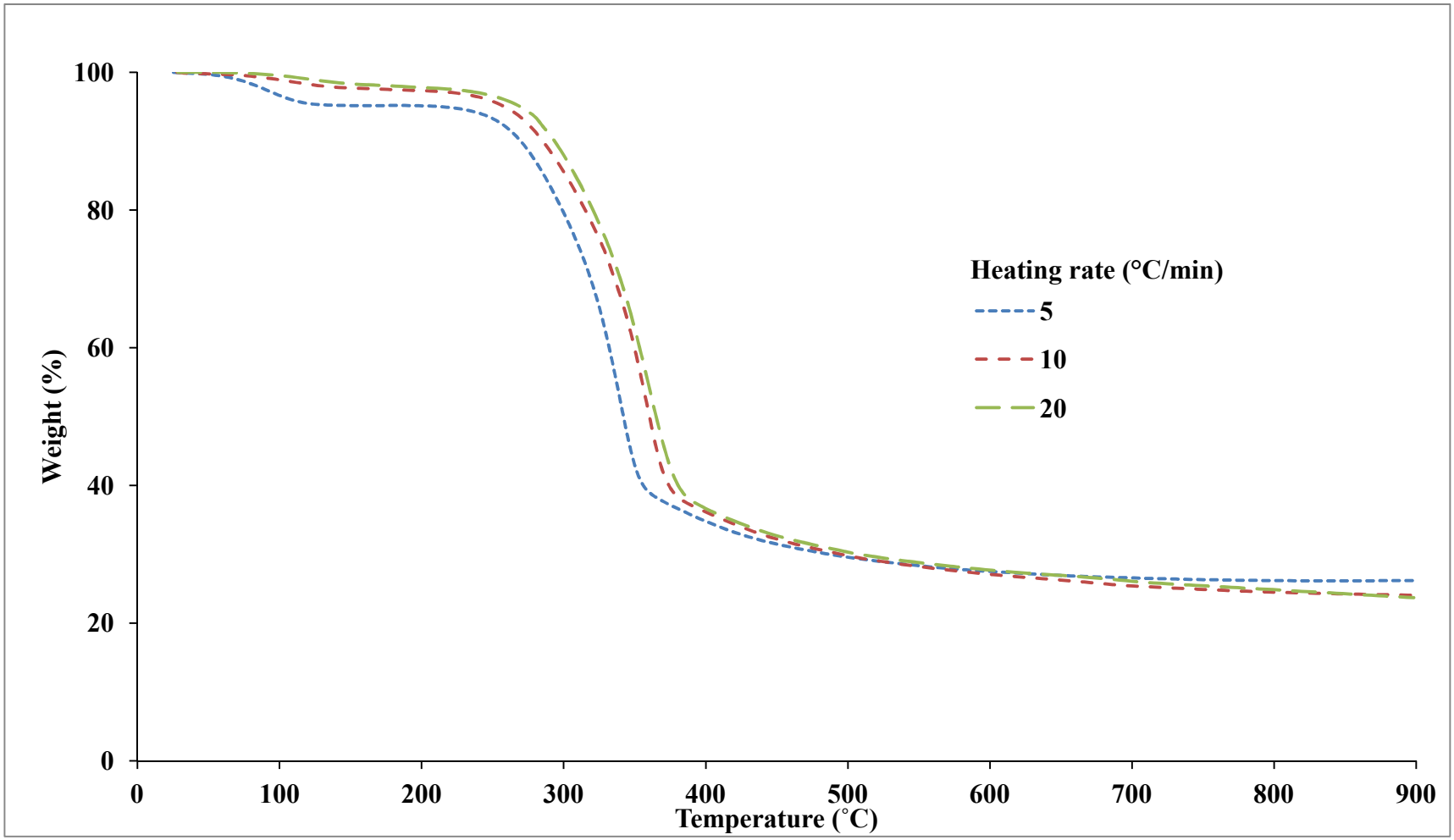

Fig. 3.1 TG curves for SS in inert atmosphere at different heating rates

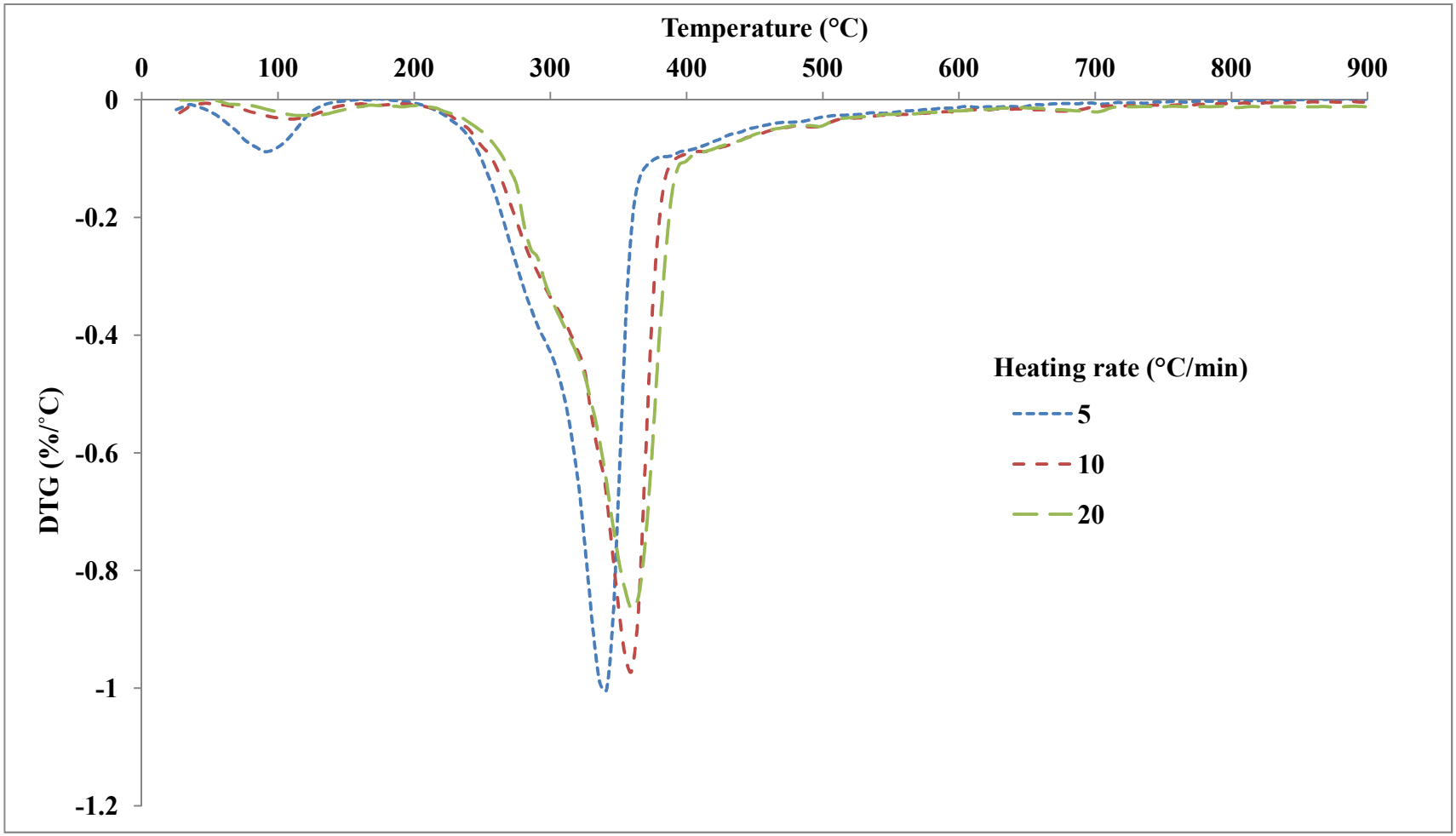

Fig. 3.2 DTG curve for SS in inert atmosphere at different heating rates

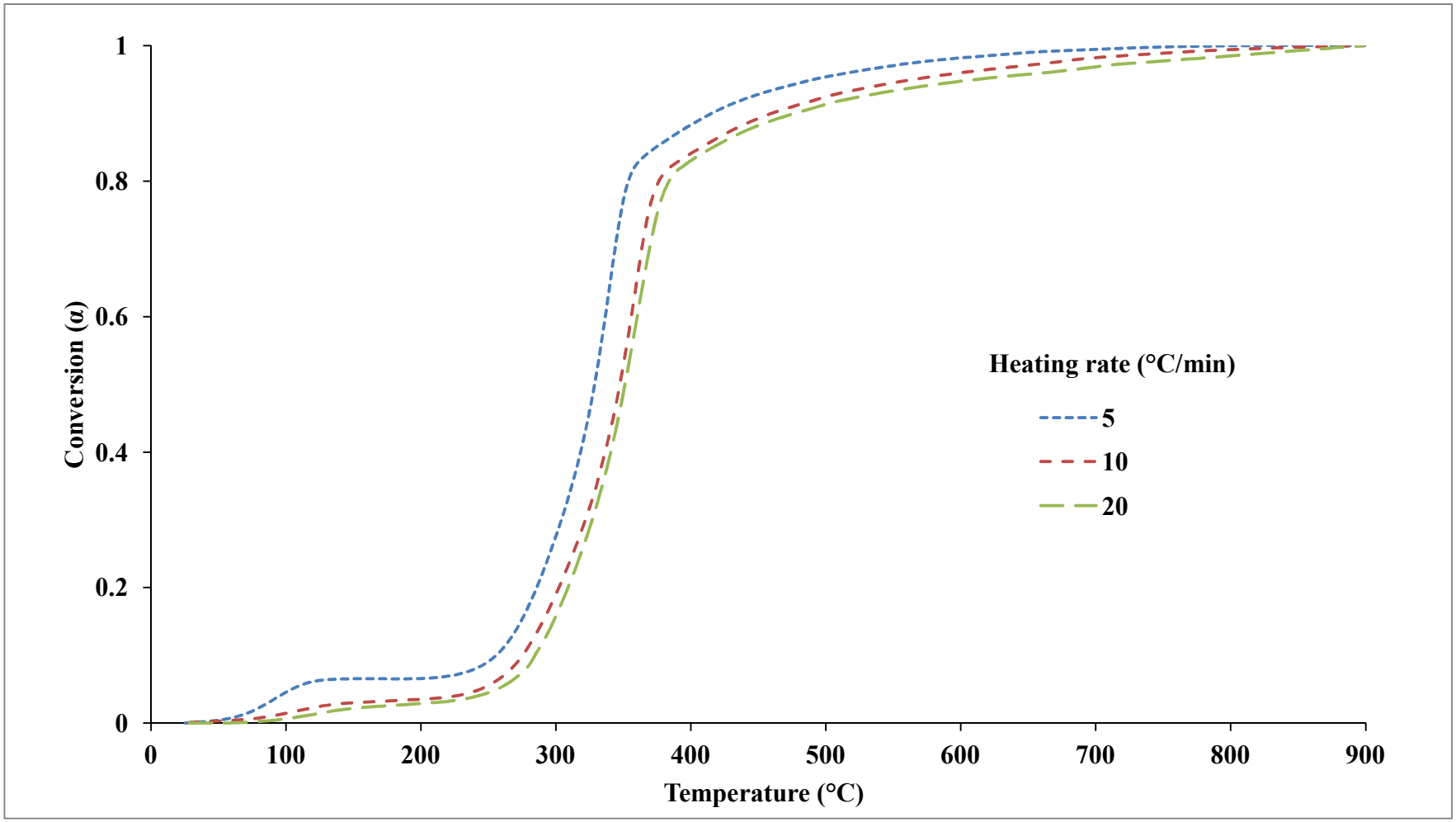

Fig. 3.3 Conversion as a function of temperature at different heating rates

3.3.3 Kinetic Study

The operation and efficient design of any thermochemical process for biofuel production from biomass requires the understanding of solid-state thermal decomposition kinetics of biomass (Turmanova et al., 2008). These multistep processes occur with different rates and also have intricate mechanism to be characterized by any simple kinetic model. Thus, to illustrate their kinetic behavior, iso-conversional models were employed in multiple steps (Vyazovkin et al., 2011).

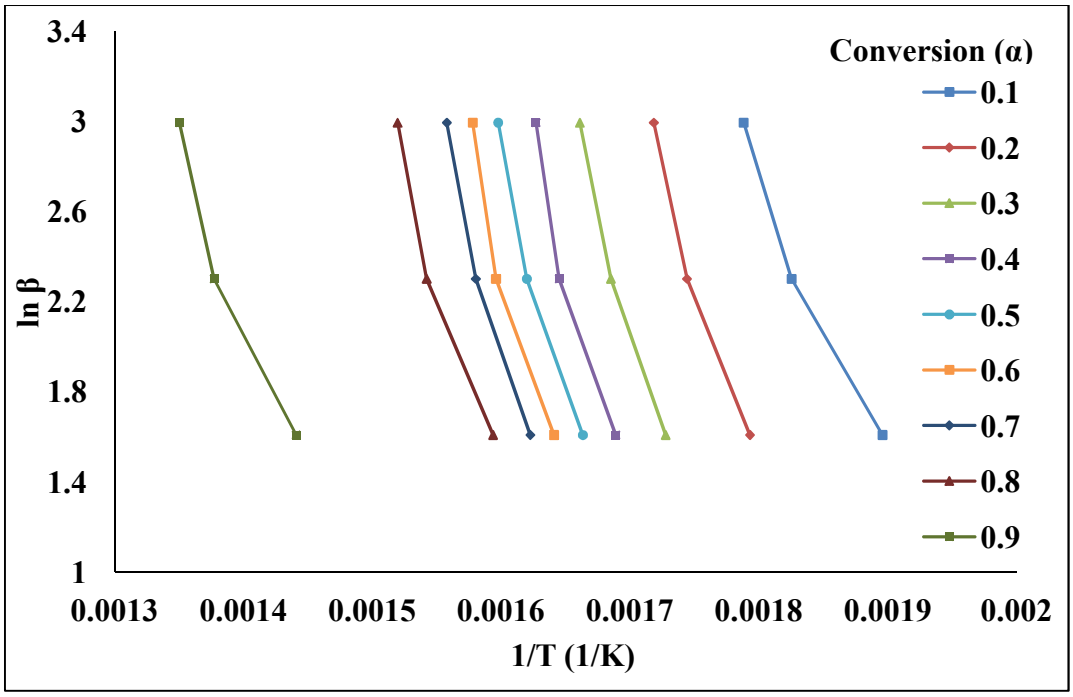

Fig. 3.4 FWO integral model for the calculation of the activation energy

In the present study, kinetic parameters were calculated by exploring the TGA experimental data. Change in biomass conversion with temperature at three different heating rates in inert atmosphere was used to calculate the temperature at each conversion for the kinetic analysis based on three different kinetic models. To reduce the effect of MC and AC, conversion varying from 0.1 to 0.9 with a step of 0.1 was used

to determine the dependence of activation energy on conversion during thermochemical process. Fig. 3.4 – 3.6 shows the plots for FWO, KAS, and Friedman iso-conversional methods used for calculating the E from their slopes with increasing conversion.

With increase in conversion the slopes of the iso-coversional plots are changing and thus E is also changing. E calculated from the above mentioned methods is presented in Table 3.3. A similar trend in the values of E with the progressive conversion was observed for all the three methods as shown in Fig. 3.7.

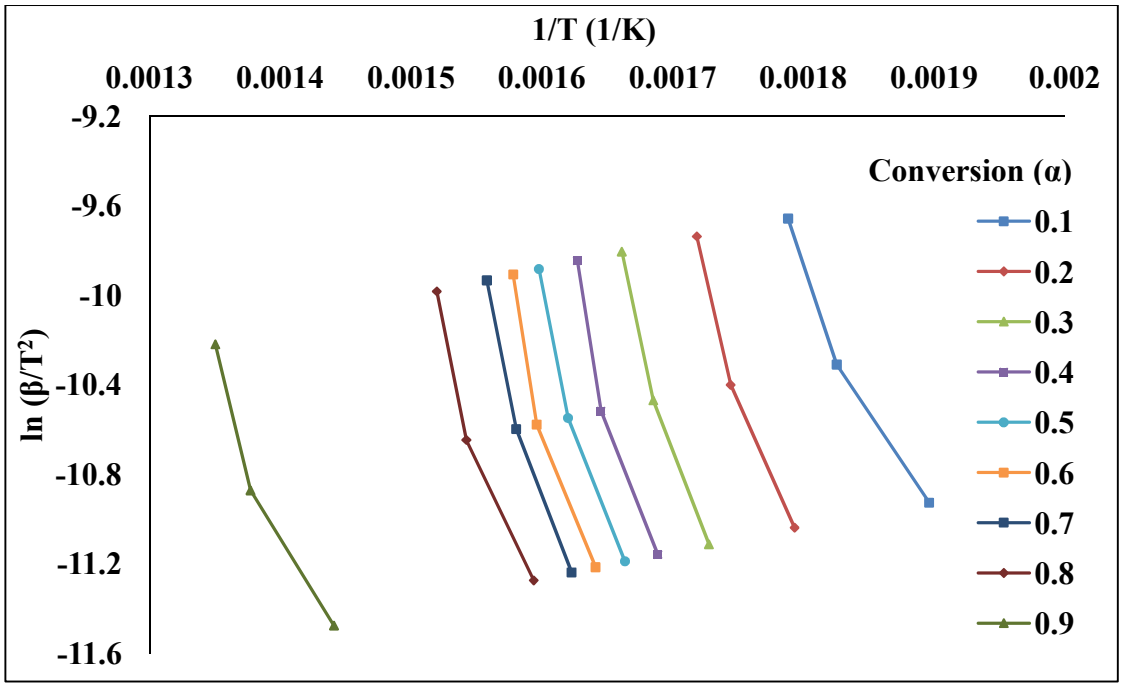

Fig. 3.5 KAS integral model for the calculation of the activation energy

For all the cases, activation first increased with conversion from 0.1 to 0.4 and then it decreased for the next 0.1 conversions. Again E was increased up to the conversion of 0.7 and then showed decreasing trend till last to a value of 114.53, 108.61, and 90.43 kJ/mol for FWO, KAS, and Friedman methods, respectively at conversion of 0.9. The co-efficient of determination (R^2) values were in between 0.9277 and 0.9914 for all

cases, indicating better fitting results. Average E for SS degradation as calculated from FWO, KAS and Friedman methods were 145.78, 143.35 and 142.87 kJ/mol, respectively. This difference in E from these three methods may be due to their different approximation and assumptions adopted (Kaur et al., 2018). For example, in case of FWO method Doyle's approximation is followed whereas Friedman method does not assume any such approximation (Yuan et al., 2017; Doyle, 1962). However, deviation of less than 2.0 % was observed in the average activation energies as obtained from three different methods. This endorses the reliability of calculations and also confirmed the predictive power of FWO, KAS and Friedman methods (Baray Guerrero et al., 2016).

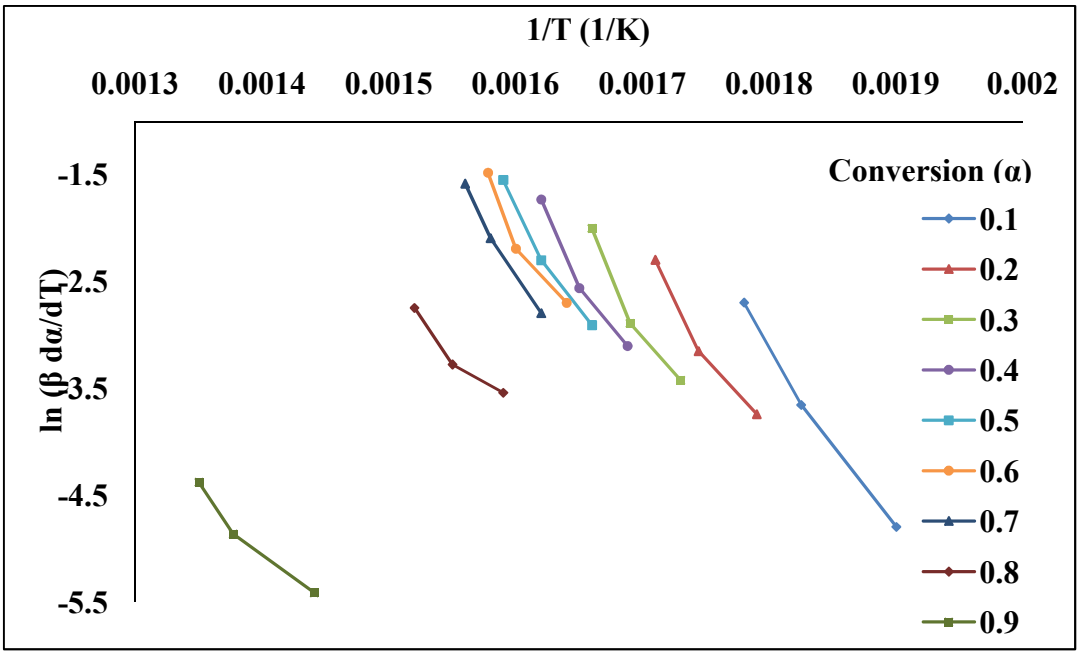

Fig. 3.6 Friedman model for the calculation of the activation energy

Kinetic study exposed the high dependence of E on conversion which denotes SS pyrolysis is a complex process consisting of different complex reactions. The average E

for SS degradation was lower than other biomass samples as presented in Table 3.4 and thus SS can be degraded to useful products at lower temperature. This lower E for the process also illustrates that SS can co-fired with other materials of lower or higher activation energies.

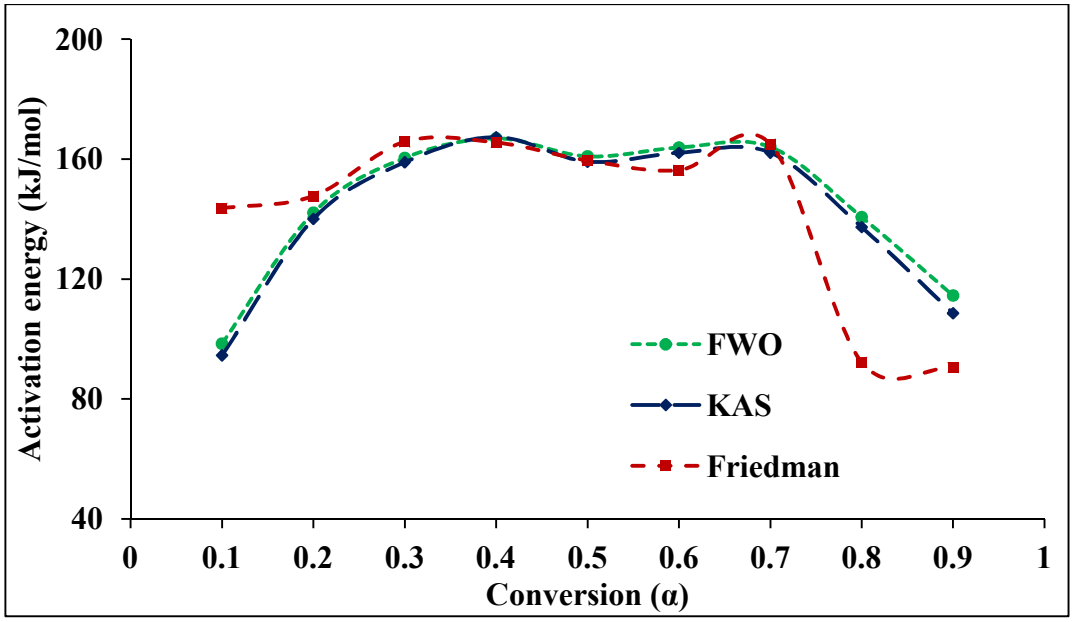

Fig. 3.7 Comparison of activation energy as a function of progressive conversion for FWO, KAS and Friedman models

However, the variation in E might be due to the simultaneous changing of reaction mechanism with progressive conversion (α) or decomposition of SS (Abyade et al., 2011). Since pyrolysis is a complex process which involves a large number of different reactions occurring simultaneously at each stage of conversion and each single stage reaction contributes to the global reaction mechanism (Xu and Chen, 2013). The reason may be that the mechanism of most solid-state reactions is not simple one-step, but complex multistep (Slopiecka et al., 2012). As the thermal degradation progresses, occurrence of secondary reactions leads to the polymerization of reacting pyrolysis

compounds that may also affect the variation in E. In addition, the variability may be due to the different pyrolysis conditions and assessment methods used for different biomasses. These results reveal the suitability of SS intended for thermochemical conversion process to produce bio-energy.

Table 3.3 Activation energy at corresponding conversion (α) for FWO, KAS and Friedman methods

Conversion (α)	FWO E (kJ/mol)	R^2	KAS E (kJ/mol)	R^2	Friedman E (kJ/mol)	R^2
0.1	98.46	0.9689	94.56	0.9632	143.57	0.9914
0.2	142.13	0.9689	140.06	0.9649	147.70	0.9638
0.3	160.40	0.9750	158.93	0.9720	165.76	0.9500
0.4	166.92	0.9446	167.30	0.9404	165.52	0.9650
0.5	160.94	0.9662	159.11	0.9620	159.49	0.9797
0.6	163.87	0.9423	162.08	0.9350	156.28	0.9326
0.7	164.06	0.9695	162.14	0.9657	164.99	0.9902
0.8	140.67	0.9515	137.32	0.9443	92.24	0.9277
0.9	114.53	0.9475	108.61	0.9370	90.43	0.9629
Average	145.78	-	143.35	-	142.87	-

Table 3.4 Comparison of activation energy of SS with other biomass

Biomass	Gas medium	Heating rate (°C/min)	Model	Average activation energy (kJ/mol)	Reference
Poplar wood	N_2	2,5,10,15	KAS FWO	158.58 157.27	(Slopiecka et al., 2012).
Oil shale	N_2	1,3,5,10,30, 50	KAS	109	(Al-Ayed et al., 2010)
Sawdust	H_2	5,10,15,20	KAS	169.94	(Park et al., 2009)
Smooth cord grass	N_2	5,10,20,40	KAS FWO Friedman	183.4 183.6 200.9	(Liang et al., 2014)
SS	N_2	5,10,20	KAS FWO Friedman	143.35 145.78 142.87	Present Study

3.3.4 Reaction mechanism

The change in E with increasing conversion signifies complex multistep reaction mechanism for the biomass degradation process (Jankovic et al. 2007). In the present study, reaction mechanism for SS degradation was assessed using Criado analysis (Z-master plot) at different conversion level at the heating rate of 10 ˚C/min. The standard

solid state reaction model used for the analysis is presented in Table 3.1. The master curves along with the experimental curve for SS degradation is depicted in Fig. 3.8.

The reaction mechanism for degradation process was decided based on the closeness of experimental curve to that of the theoretical curves. For the conversion less than 0.5 the experimental curve follows the trend of diffusion mechanism i.e. D_1, D_2, D_3 and D_4 which matches to one dimension diffusion model, two dimension diffusion model (Valenci model), three dimension diffusion (Jander model) and three dimension diffusion (Ginstlinge-Brounshtein model), respectively. At this conversion range, the domination of diffusion model may be because of high amount of VM in the SS which degrades with increasing conversion. Diffusion models are basically linked with the diffusion of products (condensable and non-condensable) and with increase in conversion, the product layer thickness around the sample increases. This thick layer around the biomass hinders the heat transfer from the external source. Thus, diffusion becomes the rate-determining step at lower conversion. However, in the conversion range from 0.5 to 0.7, experimental curve continued to follow the trend of D_3 along with Avrami-Erofeev models (A_1, A_2, A_3, and A_4) which is associated with the nucleation and growth. Finally, the experimental curve follows the trend of R_3 till conversion 0.9 which is associated with 3rd order nucleation having three nucleus on each particle. At elevated temperature, occurrence of secondary reactions leads to cracking of some ordered cellulose into chain of lower molecular mass which acts as centres for random nucleation and growth for the degradation reaction. The results showed good agreement with previous published results by Poletto et al. (2012), Mishra et al. (2015), Doddapaneni et al. (2016) and Vlaev et al. (2003).

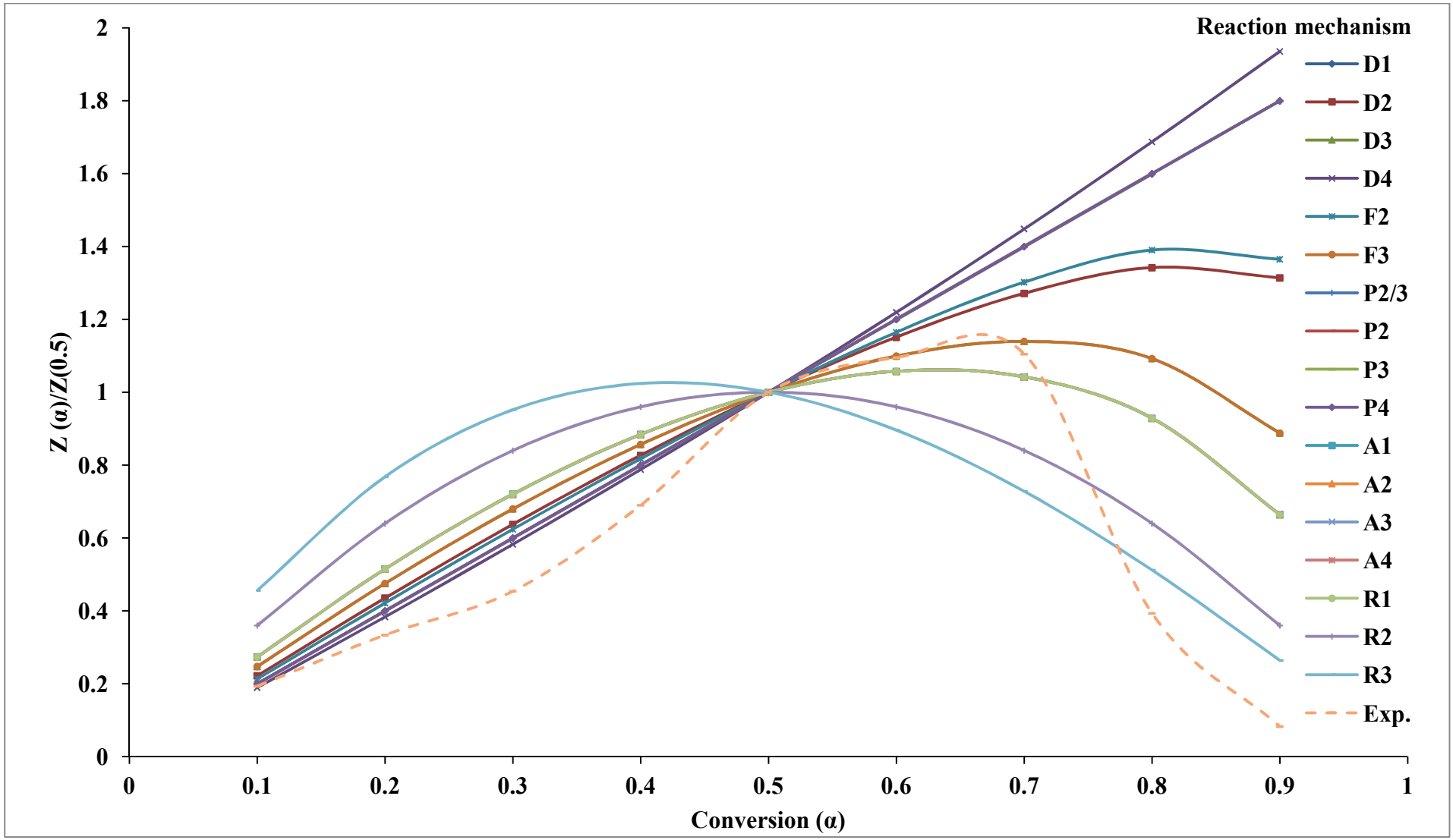

Fig. 3.8 Theoretical and experimental plots for prediction of solid state reaction mechanism using Criado method (Z-master plot)

3.3.5 Thermodynamic Study

Thermodynamic parameters (ΔH, ΔG, and ΔS) as calculated for the SS degradation process at $T = T_m$ (DTG peak temperature) for the heating rate of 10 ˚C/min is presented in Table 3.5. This T_m describes the highest rate of biomass conversion and thus it is important (Kim et al., 2010). The values of pre-exponential factor (A) were in the range of 10^5–10^{11} s^{-1} which demonstrates empirical first order pre-exponential factors. Variations in the values of A were observed as conversion progressed with increase in temperature. This may be due to the complex composition of biomass as well as complex multistep parallel reactions that occurred during degradation process (Turmanova et al., 2008). The values of A for SS ranged from 6.40×10^5 to 4.76×10^{11} s^{-1}. The lower values of A and E denotes an easier and faster decomposition of biomass at corresponding conversion (Yuan et al., 2017). Higher value of A symbolizes occurrence of slower reaction. These values for SS are comparatively lower and can be treated thermochemically for bioenergy production. The value for A less than 10^9 indicates surface reaction or closed complex and high factors ($\geq 10^9$ s^{-1}) indicates simple complex. The values of A in the range 10^9 –10^{11} proclaim that activated complex was confined in rotation to the initial substance (Vlaev et al., 2007).

The ΔS measure the randomness (disorder) in a system and is summarized in Table 3.5. The ΔS for SS degradation varied from -147.21 to -35.59 J/mol, which were higher in comparison to rice straw and rice bran -4.13 and -62.14 J/mol, respectively (Sharma et al., 2015). All the values are negative indicating fickleness of the products obtained after bond disengagement was lower than that of initial substance. Negative values of the entropy of formation of complex illustrate activated complex can be characterized by a higher degree of arrangement, i.e. activated complex has more organized structure than initial material.

Table 3.5 Thermodynamic parameters for SS degradation at the heating rate of 10 °C/min

Conversion (α)	E (kJ/mol)	A (1/s)	ΔH (kJ/mol)	ΔG (kJ/mol)	ΔS (J/mol.K)
0.1	98.46	6.40×10^{5}	93.91	187.21	-147.21
0.2	142.13	3.67×10^{9}	137.36	185.28	-75.61
0.3	160.40	1.33×10^{11}	155.46	184.63	-46.02
0.4	166.92	4.76×10^{11}	161.87	184.43	-35.59
0.5	160.94	1.48×10^{11}	155.81	184.61	-45.44
0.6	163.87	2.62×10^{11}	158.66	184.53	-40.82
0.7	164.06	2.72×10^{11}	158.80	184.52	-40.58
0.8	140.67	2.75×10^{9}	135.28	185.34	-79.03
0.9	114.53	1.57×10^{7}	108.49	186.42	-122.96
Average	**145.76**	**-**	**140.63**	**185.22**	**-70.36**

The ΔS for the system reflect how the system is related to its own thermodynamic equilibrium. In low activation entropy material just passes through some physical and chemical aging process, bringing it to a state of its own thermodynamic equilibrium. In this condition, larger time is required to form an activated complex as material has little

reactivity. On the contrary when high activation entropy values are observed, material is far from its thermodynamic equilibrium and thus the reactivity is high resulting faster formation of the activated complex (Filho and Curti, 2006). According to Daugaard and Brown, (2003), enthalpy for biomass pyrolysis is the energy consumed by biomass to raise its temperature from ambient to the reaction temperature and convert the biomass to reaction products (gas, liquid, and biochar). The change in enthalpy (ΔH) describes the energy difference between the activated complex and the reagents. If this difference is small (4 – 5 kJ/mol) then potential energy barrier is low, thus, the formation of activated complex is favored (Malika, et al., 2016). The average change in enthalpy of the process was 140.63 kJ/mol whereas average enthalpies for other biomass like castor seed (Kaur, et al., 2018), Para grass (Ahmad et al., 2017), rice straw and dairy manure (Xu and Chen, 2013) were 162.15, 173.66, 162.23, and 153.10 kJ/mol, respectively. The positive value for ΔH signifies the requirement of energy for the formation of products from the biomass degradation. It also indicates that the process is endothermic. Although the process is endothermic but this enthalpy value is much lower and can be considered thermo neutral depending upon the deign parameters of the system (Daugaard and Brown, 2003).

The change of Gibbs free energy (ΔG) is influenced by other two thermodynamic parameters, i.e. ΔH and ΔS. The ΔG varied from 184.43 to 187.21 kJ/mol for SS degradation. This ΔG illustrates the total energy enhancement of the system at the approach of the reagents and the activated complex formation (Sheng et al., 2014). These findings illustrate SS has enormous quantity of inherent energy and enough potential for bio-energy generation.

3.4 Conclusions

In this study, thermal degradation of SS has been examined under nitrogen atmosphere by means of TGA at different heating rates (5, 10, and 20 ˚C/min). Effect of heating rates on TG and DTG curve is well presented and with increase in heating rate, maximum weight loss peak shifted to a higher temperature. Maximum devolatilization of SS took place in the temperature range of 210 – 500 ˚C. The activation energies as calculated from different iso-conversional models (FWO, KAS, and Friedman) were 143.35, 145.78, and 142.87 kJ/mol and confirmed that E is not linearly dependent on conversion. Change in E with increasing conversion indicated multi step kinetics for SS degradation process. High VM content and low MC and AC make SS an innovative back up source for the production of biofuel and chemicals. This kinetic data will provide an important guideline for the design and development of thermochemical process for SS. The results obtained from the study are vital as this will contribute for future application of SS as waste to renewable energy source.

Based on the kinetics and thermodynamic study discussed above, the next chapter presents the salient findings of effect of process parameters on pyrolysis products yield and characteristics.